

Association of a Novel Mutation in the *Plasmodium falciparum* Chloroquine Resistance Transporter With Decreased Piperaquine Sensitivity

Sonia Agrawal,¹ Kara A. Moser,² Lindsay Morton,¹ Michael P. Cummings,³ Ankita Parihar,² Ankit Dwivedi,² Amol C. Shetty,² Elliott F. Drabek,^{2,a} Christopher G. Jacob,^{1,a} Philipp P. Henrich,⁷ Christian M. Parobek,⁶ Krisada Jongsakul,⁹ Rekol Huy,⁵ Michele D. Spring,⁹ Charlotte A. Lanteri,^{9,a} Suwanna Chaorattanakawee,^{9,10} Chanthap Lon,^{4,9} Mark M. Fukuda,⁹ David L. Saunders,⁹ David A. Fidock,^{7,8} Jessica T. Lin,⁶ Jonathan J. Juliano,⁶ Christopher V. Plowe,¹ Joana C. Silva,² and Shannon Takala-Harrison¹

¹Division of Malaria Research, Institute for Global Health, and ²Institute for Genome Sciences, University of Maryland School of Medicine, Baltimore; ³Center for Bioinformatics and Computational Biology, University of Maryland, College Park; ⁴Armed Forces Research Institute of Medical Sciences, and ⁵National Center for Parasitology Entomology and Malaria Control, Phnom Penh, Cambodia; ⁶Division of Infectious Diseases, University of North Carolina at Chapel Hill; ⁷Department of Microbiology and Immunology, and ⁸Division of Infectious Diseases, Department of Medicine, Columbia University Medical Center, New York; ⁹Armed Forces Research Institute of Medical Sciences, Department of Immunology and Medicine, and ¹⁰Department of Parasitology and Entomology, Faculty of Public Health, Mahidol University, Bangkok, Thailand

Background. Amplified copy number in the *plasmepsin II/III* genes within *Plasmodium falciparum* has been associated with decreased sensitivity to piperaquine. To examine this association and test whether additional loci might also contribute, we performed a genome-wide association study of ex vivo *P. falciparum* susceptibility to piperaquine.

Methods. *Plasmodium falciparum* DNA from 183 samples collected primarily from Cambodia was genotyped at 33 716 genome-wide single nucleotide polymorphisms (SNPs). Linear mixed models and random forests were used to estimate associations between parasite genotypes and piperaquine susceptibility. Candidate polymorphisms were evaluated for their association with dihydroartemisinin-piperaquine treatment outcomes in an independent dataset.

Results. Single nucleotide polymorphisms on multiple chromosomes were associated with piperaquine 90% inhibitory concentrations (IC₉₀) in a genome-wide analysis. Fine-mapping of genomic regions implicated in genome-wide analyses identified multiple SNPs in linkage disequilibrium with each other that were significantly associated with piperaquine IC₉₀, including a novel mutation within the gene encoding the *P. falciparum* chloroquine resistance transporter, PfCRT. This mutation (F145I) was associated with dihydroartemisinin-piperaquine treatment failure after adjusting for the presence of amplified *plasmepsin II/III*, which was also associated with decreased piperaquine sensitivity.

Conclusions. Our data suggest that, in addition to *plasmepsin II/III* copy number, other loci, including *pfcr*, may also be involved in piperaquine resistance.

Keywords. malaria; piperaquine; resistance; *Plasmodium falciparum*; chloroquine resistance transporter; plasmepsin.

Artemisinin-based combination therapies (ACTs) are used worldwide and have contributed to reductions in the malaria burden in many areas. In response to inadequate efficacy of ACTs such as artesunate-mefloquine and artemether-lumefantrine [1, 2], dihydroartemisinin-piperaquine became the drug of choice to treat multidrug-resistant *Plasmodium falciparum* in regions of Southeast Asia plagued by artemisinin resistance. In

addition, dihydroartemisinin-piperaquine is being used in field evaluations of targeted mass treatment to eliminate malaria within the Greater Mekong subregion in hopes of arresting the spread of resistance [3]. However, dihydroartemisinin-piperaquine efficacy rates as low as 46% have been reported in regions of western Cambodia where artemisinin resistance is well established [4–6], and decreased in vitro piperaquine susceptibility has been seen in parasites collected from these areas [7, 8]. These findings suggest the emergence of piperaquine resistance in addition to existing artemisinin resistance, which bodes poorly for the ability to treat *P. falciparum* in this part of the world.

Molecular assays to detect markers of antimalarial drug resistance are valuable surveillance tools. Mutations within PfKelch13 have been identified and genetically confirmed as markers of resistance to the artemisinins [9–11]. Two recent studies have indicated that copy number variation in the *plasmepsin II* and *III* genes, located on chromosome 14 of *P. falciparum*, may serve as a molecular marker for decreased piperaquine sensitivity [12, 13];

Received 24 May 2017; editorial decision 10 July 2017; accepted 12 July 2017; published online July 17, 2017.

Presented in part: Annual Meeting of the American Society of Tropical Medicine and Hygiene, Philadelphia, Pennsylvania, November 2015. Presentation number: LB-5375.

^aPresent affiliation/address: Atreca, Inc., Redwood City, California (E. F. D.); Wellcome Trust Sanger Institute, Hinxton, United Kingdom (C. G. J.); Uniformed Services University of the Health Sciences, Rockville, Maryland (C. A. L.).

Correspondence: S. Takala-Harrison, PhD, Division of Malaria Research, Institute for Global Health, University of Maryland School of Medicine, 685 W Baltimore St, HSF1-480, Baltimore, MD 21201 (stakala@som.umaryland.edu).

The Journal of Infectious Diseases® 2017;216:468–76

© The Author 2017. Published by Oxford University Press for the Infectious Diseases Society of America. All rights reserved. For permissions, e-mail: journals.permissions@oup.com. DOI: 10.1093/infdis/jix334

however, other loci may be involved. Using samples collected from Cambodia, we performed a genome-wide association study of ex vivo *P. falciparum* susceptibility to piperazine to identify candidate resistance loci. Here we report that in addition to *plasmepsin II/III* copy number, other loci are associated with decreased piperazine sensitivity, including a novel mutation within the *pfCRT* gene.

METHODS

Study Samples

Samples used in the genome-wide association study were collected from individuals with clinical malaria participating in 1 of the 3 following studies (Supplementary Table 1): (1) a clinical trial of artesunate conducted in Battambang province from 2006–2007 ($n = 30$) [14]; (2) a malaria survey conducted from 2009–2014 in 8 Cambodian provinces: Battambang, Pailin, Koh Kong, Kampot, Kampong Speu, Oddar Meanchey, Preah Sihanouk, and Preah Vihear ($n = 145$) [7]; and (3) a single-arm clinical evaluation of artesunate-mefloquine conducted in Kanchanaburi province, Thailand ($n = 8$). One hundred eighty-three samples had both genotypes and phenotypes available.

Samples used in the validation dataset ($n = 53$) were collected as part of a therapeutic efficacy study conducted in Oddar Meanchey province that assessed the efficacy of a 3-day course of dihydroartemisinin-piperazine [5]. In this study, using polymerase chain reaction (PCR) genotyping of *P. falciparum* *msp1*, *msp2*, and *glurp*, the PCR-adjusted 42-day recrudescence rate was found to be 54% by modified intention-to-treat analysis [5].

Samples were collected under informed consent as approved by the Walter Reed Army Institute of Research and local in-country institutional review boards and were approved for use by the University of Maryland School of Medicine.

Parasite Genotypes

DNA extracted from leukocyte-depleted venous blood was genotyped using a *P. falciparum*-specific NimbleGen 4.2M probe DNA microarray that types a total of 33 716 single nucleotide polymorphisms (SNPs) [15]. One hundred seventeen isolates also underwent whole-genome sequencing using Illumina HiSeq 2000, using 101 base pair-paired end reads, without prior amplification. Illumina sequencing was also performed separately at the University of North Carolina to generate whole-genome sequence data for the 53 additional samples used as a validation dataset [16]. Statistics describing the breadth of genome coverage and read depth for both datasets can be found in Supplementary Table 2. Single nucleotide polymorphism calling for both datasets was performed at University of Maryland following Genome Analysis Toolkit's best practices [17–19] using Unified Genotyper v3.1.1. Single nucleotide polymorphisms were filtered on phred-based quality score, read depth, strand bias, and mapping quality to generate a high-confidence SNP

call set. The SNP array data have been submitted to the National Institutes of Health Gene Expression Omnibus for public access (www.ncbi.nlm.gov/geo/; accession number: GSE100704). Whole genome sequences were submitted to GenBank (accession numbers: SAMN06175892–SAMN06176015).

Phenotype

Ex vivo piperazine 90% inhibitory concentrations (IC_{90} s) were assessed using a histidine-rich protein-2 enzyme-linked immunosorbent assay (HRP-2 ELISA) as previously described [20, 21]. All assays were performed in the same laboratory at the Armed Forces Research Institute of Medical Science [21]. Piperazine concentrations in the assay ranged 0.9–674 nM, including a no drug control. In 2013, we began to observe isolates with the ability to grow in the maximum concentration of drug used in the standard range. As a result, starting in 2014, an increased range of piperazine concentrations (3.4–53 905 nM) was used in addition to the standard dilutions. To estimate piperazine IC_{90} of parasites that grew in the maximum concentration of drug from the standard range (0.9–674 nM), the curves were replotted by fitting “zero-growth” HRP-2 optical density values at the extrapolated piperazine concentration of 53 905 nM. Dose–response curves for isolates with a range of susceptibilities have been described previously [20, 22]. Ninety percent inhibitory concentration was used as the phenotype because it was better correlated with treatment outcome in our validation dataset and in other studies [20] compared with IC_{50} . A recent article also reported that IC_{90} values were more reliable than IC_{50} values when quantifying differences in piperazine susceptibility [23]. The piperazine survival assay [8] was not performed on isolates included in this study.

ADMIXTURE Analysis and Single Nucleotide Polymorphism Imputation

ADMIXTURE 1.23 [24] was used to group parasites into subpopulations for the purpose of imputation and to adjust for confounding in the association analysis. The number of subpopulations, K , was varied from 1 to 15, with 10 replicate runs per K . Cross-validation errors were used to determine the appropriate K . Parasites clustered into 6 subpopulations. Ancestry values were used from the replicate with the greatest log-likelihood, and isolates were assigned to a subpopulation based on their greatest ancestry value (Supplementary Figure 1).

Beagle version 3.3.2 [25] was used to impute missing SNP calls for all isolates included in the genome-wide association analysis. Missing SNP calls were not imputed for whole-genome sequences in the fine-mapping analysis of genomic regions identified in the genome-wide association analysis. A 2-step approach was applied to impute the missing genotypes. Parasites with 100% ancestry values in each subpopulation were imputed within that subpopulation, and these imputed “pures” were used as a reference set to impute admixed parasites. A genotype probability of 90% was used to call an imputed SNP.

Quality Control

The proportion of missing SNP calls was plotted by SNP and by sample. Invariant nucleotide positions across 183 samples, SNPs with >40% missing calls, and samples with >40% missing calls were excluded before analysis. These criteria resulted in the removal of 28 253 SNPs (23 271 invariant SNPs and 4982 with a high proportion of missing calls) and 30 samples. An additional 2751 SNPs with minor allele frequency <5% were removed before analysis. After quality control, the final genome-wide association analysis included 2712 SNPs and 153 samples.

Correspondence Between Genetic Subpopulations

A hierarchical clustering approach using a proportional distance matrix, performed on previously published *P. falciparum* sequences from Cambodia [26] (Dwivedi et al, submitted), was used to determine the correspondence between genetic subpopulations in this study and those from the Dwivedi study. A total of 2474 SNPs from 320 samples (153 from this study and 167 from the Dwivedi study) were used in the analysis. Dwivedi and colleagues have shown that stable clusters can be obtained with as few as 1000 SNPs. The correspondence between the subpopulations is shown in Supplementary Figures 2 and 3.

Regression

Genome-wide mixed model association (GEMMA) [27] was used to estimate the association between each SNP and \log_{10} -transformed piperaquine IC_{90} (treated as a continuous variable), adjusting for genetic subpopulation, the presence of mutations in the *kelch13* gene, and the first 3 principal components of a principal components analysis. Principal components were estimated from a matrix of pair-wise sample identity-by-state metrics [28]. An identity-by-state allele-sharing matrix was included as a random effect to account for the correlation between genetically similar individuals that results from population structure. The GEMMA method was used to estimate coefficients and *P* values. A Bonferroni threshold (0.05/number of SNPs analyzed) was used to evaluate genome-wide significance. Quantile-quantile plots for *P* values were used to assess the robustness of modeling approaches in minimizing false-positive results due to population structure or other confounding.

Random Forests

Random forest analyses [29] were done using the randomForest package [30] of the R statistical computing environment [31]. Because there is not an explicit way to control for confounding due to population structure in random forests, analysis was performed within the genetic subpopulation containing most parasites with the highest IC_{90} values (subpopulation 2, *n* = 22). The number of variables tested at each split ranged 323–1097, and the number of trees in the forest was 100 000. The importance of each SNP in predicting log-transformed piperaquine

IC_{90} (treated as a continuous variable) was assessed based on the percentage increase in mean-squared error.

Linkage Disequilibrium

The program Haploview [32] was used to determine linkage disequilibrium (LD) around SNPs associated with piperaquine susceptibility in genome-wide analyses. Linkage disequilibrium windows were defined to include all SNPs upstream and downstream of the associated SNP or mutation of interest up to but not including the next SNP with minor allele frequency (MAF) > 0.05 and R^2 < 0.3. For associated SNPs, LD windows (Supplementary Table 3) were defined within parasites with the highest IC_{90} values (ie, $\log_{10} IC_{90} > 3.0$) in genetic subpopulation 2 to avoid false LD estimates due to population structure.

Gene Copy Number Analysis

Copy number variation was assessed across the 117 samples for which whole-genome sequences were generated. Raw paired-end sequences from each sample were aligned against the *P. falciparum* 3D7 (PlasmoDB version 24) reference sequence using bowtie2 (version 2.2.4) [33]. For each sample, we calculated the number of reads that overlap known coding sequence intervals based on the *P. falciparum* 3D7 reference annotation general feature format file. The overlapping reads for each sample were normalized by mean coverage of the sample. Gene coverage in *P. falciparum* telomeric and internal hypervariable repeat regions [34] was excluded. Linear regression was used to model normalized coverage of *P. falciparum* core genes as a function of log-transformed piperaquine IC_{90} . To estimate the number of copies of the *plasmepsin II* and *III* genes within samples with whole genome sequence data, copy number variations across chromosome 14 were determined by applying a previously described procedure [34].

Association With Treatment Outcome

Cox proportional hazards was used to model the time to *P. falciparum* recurrence in individuals with a given mutation (eg, PfCRT F145I or amplified *plasmepsin II/III* copy number) compared with those without that mutation in the independently sequenced validation dataset. Hazard ratios (HRs) and 95% confidence intervals (CIs) were estimated using SAS v.9.3.

RESULTS

A total of 183 samples had both SNP array data and ex vivo phenotypes available (Supplementary Table 1). After quality control, a total of 2712 SNPs and 153 samples were included in the final genome-wide association analysis. Of these 153 samples, 117 successfully underwent whole-genome sequencing for use in fine-mapping and copy number variation analyses.

Phenotype Distribution

The distribution of log-transformed piperaquine IC_{90} s is shown in Figure 1 (Supplementary Table 4). Parasites with the highest IC_{90} s

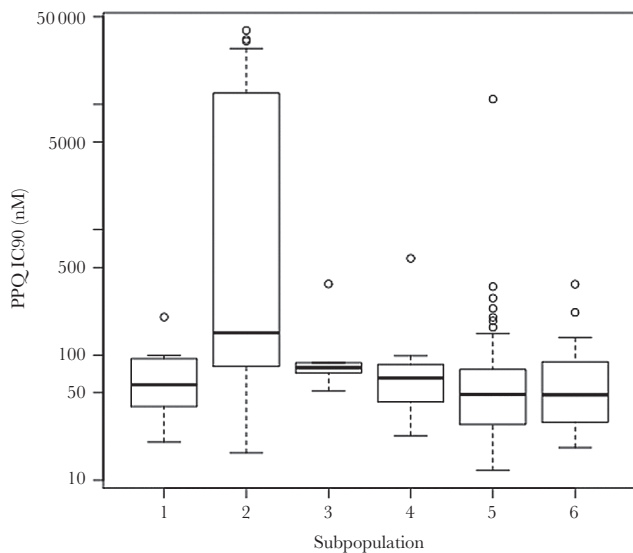


Figure 1. Distribution of piperazine 90% inhibitory concentrations (IC_{90}) by genetic subpopulation. Parasites in the genome-wide analysis grouped into 6 genetic subpopulations. Most parasites with elevated piperazine IC_{90} s grouped together in genetic subpopulation 2 ($n = 22$). Abbreviations: IC_{90} , 90% inhibitory concentration; PPQ, piperazine.

clustered into the same genetic subpopulation (subpopulation 2, $n = 22$). Parasites from subpopulation 2 corresponded with the artemisinin-resistant KH2.2 subpopulation from a study conducted by Dwivedi and colleagues (Dwivedi et al, submitted) (Supplementary Figure 2). No parasites from this study corresponded with the artemisinin-sensitive ancestral Southeast Asian subpopulation KH1.1 from the Dwivedi study (Supplementary Figure 3).

Genome-Wide Associations

Ten SNPs on chromosomes 6, 10, 11, 12, and 14 achieved genome-wide significance in linear mixed models of the

association between each SNP on the array and piperazine IC_{90} (Figure 2). The random forests analysis identified an SNP on chromosome 11 as the best predictor of piperazine IC_{90} (MAL11:1816380), with SNPs on chromosomes 7, 8, 9, 10, and 14 also being among the top predictors of log-transformed IC_{90} (Figure 3). All SNPs from the array that were associated with piperazine susceptibility are shown in Supplementary Table 5.

Fine-Mapping Using Whole-Genome Sequences

Regions of LD are defined for each SNP in Supplementary Table 5 (Supplementary Table 3). From these regions of the genome, all SNPs identified in parasites that underwent whole-genome sequencing were included in linear mixed models of the association between log-transformed piperazine IC_{90} and each locus. Nineteen SNPs, many of which were in perfect LD with each other, achieved genome-wide significance and had a positive coefficient (ie, the nonreference allele was associated with the phenotype) (Table 1). These loci included the SNP encoding a mutation at position 145 within the *pfert* gene (F145I), SNPs within a large region of chromosome 10, and SNPs on chromosomes 9 and 14. Based on gene ontology classification in PlasmoDB, only 1 gene in Table 1, *pfert*, has a predicted function related to drug response, transport, or hemoglobin metabolism.

Copy Number Analysis

Linear regression was used to model normalized read coverage of *P. falciparum* core genes as a function of log-transformed piperazine IC_{90} in samples for which whole-genome sequence was available ($n = 117$). Read coverage of 2 genes on chromosome 14, *plasmepsin II* and *III*, showed the strongest association with piperazine IC_{90} (Figure 4). Read coverage of the *pfmdr1* gene was not significantly associated with piperazine IC_{90} after accounting for multiple comparisons ($P = .01$).

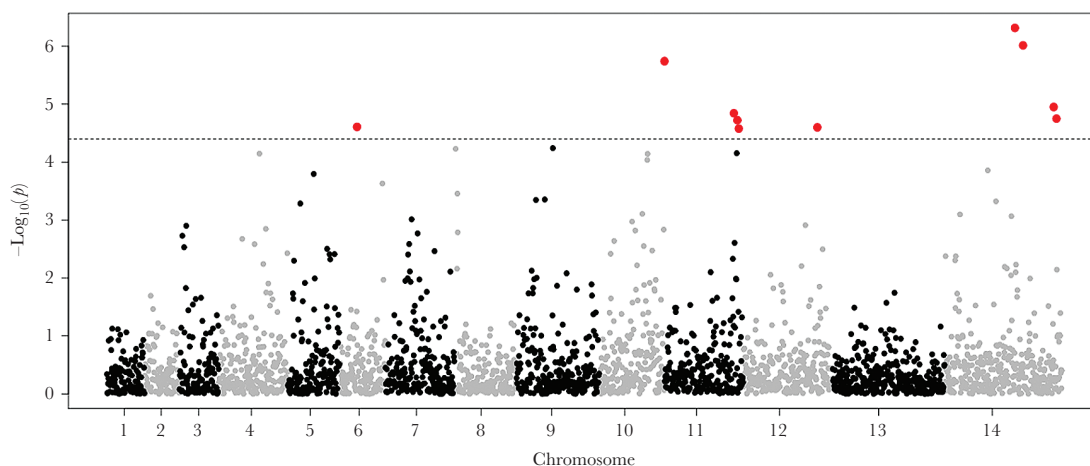


Figure 2. Manhattan plot of the association between genome-wide parasite genotypes and piperazine 90% inhibitory concentrations (IC_{90}). Linear mixed models were used to estimate the association between single nucleotide polymorphisms (SNPs) on the DNA microarray and a continuous measure of log-transformed piperazine IC_{90} ($n = 153$). The SNPs achieving genome-wide significance are shown in red. The SNPs on chromosomes 6, 10, 11, 12, and 14 were significantly associated with the phenotype. The SNP in *PfCRT* encoding the F145I mutation was not included in the microarray and was only detected by whole-genome sequencing.

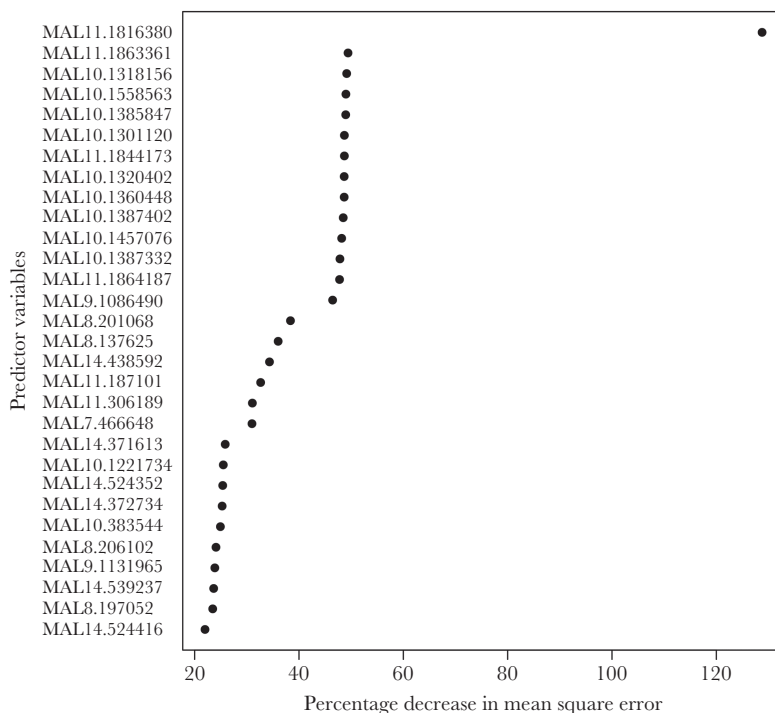


Figure 3. Random forest variable importance plot identifying loci from the DNA microarray that best predict piperazine 90% inhibitory concentrations (IC_{90}). Random forests were used to identify loci that were the best predictors of a continuous measure of log-transformed piperazine IC_{90} in samples from genetic subpopulation 2 ($n = 22$). The single nucleotide polymorphisms (SNPs) showing the greatest percentage increase in mean squared error (x-axis) are the best predictors of the phenotype. The SNPs on chromosomes 7, 8, 9, 10, 11, and 14 were the top predictors of log-transformed IC_{90} .

Table 1. Single Nucleotide Polymorphisms Associated With Piperazine 90% Inhibitory Concentrations in Fine-Mapping Analysis of Whole-Genome Sequence Data

SNP	Gene (mutation)	P value
MAL7:404010	PF3D7_0709000 (Chloroquine resistance transporter, F145I)	3.61E-07
MAL9:1233153	PF3D7_0930800 (Conserved membrane protein, T2490I)	3.61E-07
MAL9:1233160	PF3D7_0930800 (Conserved membrane protein, 2492S)	3.61E-07
MAL9:1279569	PF3D7_0932100 (Conserved membrane protein, intronic)	3.61E-07
MAL9:1279572	PF3D7_0932100 (Conserved membrane protein, intronic)	3.61E-07
MAL10:1318156	PF3D7_1032900 (RNA polymerase II-associated protein 1, 932L)	8.75E-07
MAL10:1343706	PF3D7_1033500 (WD repeat-containing protein 70, I687M)	3.61E-07
MAL10:1351775	PF3D7_1033800 (Plasmepsin VII, intronic)	3.61E-07
MAL10:1362218	PF3D7_1034100 (Conserved protein, 118G)	3.61E-07
MAL10:1369153	PF3D7_1034400 (Flavoprotein subunit of succinate dehydrogenase, Q13K)	3.61E-07
MAL10:1372810	PF3D7_1034500 (Conserved protein, C651Y)	3.61E-07
MAL10:1391842	PF3D7_1035100 (Probable protein, D133A)	3.61E-07
MAL10:1392054	PF3D7_1035100 (Probable protein, S204R)	3.61E-07
MAL10:1400026	PF3D7_1035300 (Glutamate-rich protein, P278S)	3.61E-07
MAL10:1401296	PF3D7_1035300 (Glutamate-rich protein, S701F)	3.61E-07
MAL10:1506404	PF3D7_1038000 (Antigen UB05, 51I)	3.61E-07
MAL10:1546332	PF3D7_1038400 (Gametocyte-specific protein,)	3.61E-07
MAL10:1552425	PF3D7_1038600 (Exported protein, H210R)	3.61E-07
MAL14:408912	PF3D7_1410300 (WD repeat-containing protein, 2717P)	3.61E-07

Linear mixed models were used to estimate the association between single nucleotide polymorphisms (SNPs) identified in regions of the genome in linkage disequilibrium with loci from Supplementary Table S5 and a continuous measure of log-transformed piperazine 90% inhibitory concentrations (IC_{90}) in samples that underwent whole-genome sequencing. The SNP corresponding to PfCRT F145I is shown in bold text and was the only locus with gene ontology terms suggesting a function in hemoglobin metabolism, drug response, or transport.

Abbreviation: SNP, single nucleotide polymorphism.

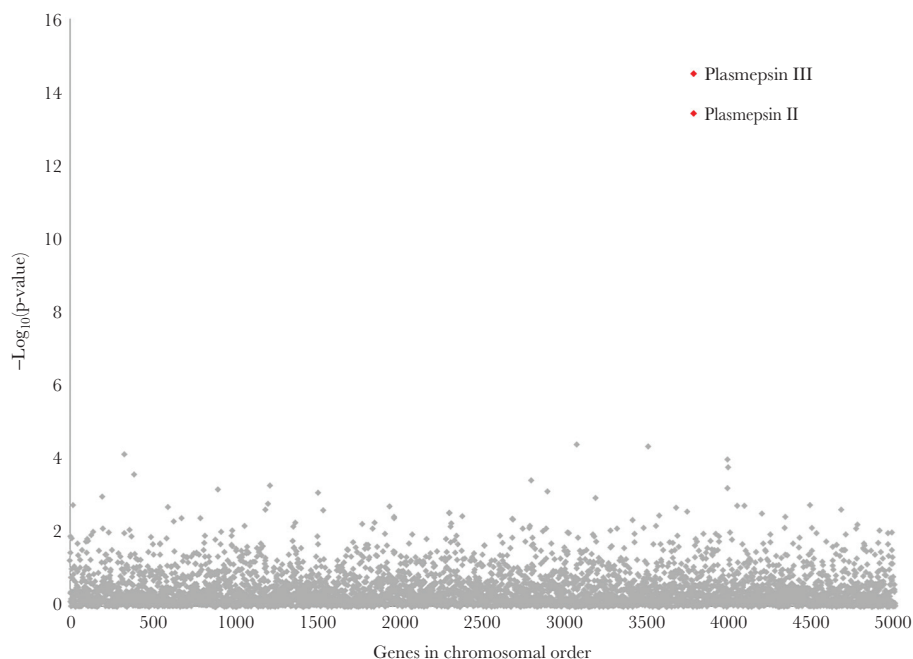


Figure 4. Association between gene copy number and piperazine 90% inhibitory concentrations (IC_{90}). Linear regression was used to model normalized coverage of *Plasmodium falciparum* core genes in 117 whole-genome sequences as a function of log-transformed piperazine IC_{90} (treated as a continuous variable). Normalized coverage of the *plasmepsin II/III* genes showed the strongest association with piperazine IC_{90} (P values indicated in red).

Validation Dataset

To validate the observed associations, we examined sequences generated from parasites collected during a study evaluating the therapeutic efficacy of dihydroartemisinin-piperazine ($n = 53$) [5]. In this independent dataset, the unadjusted hazard of *P. falciparum* recurrence in patients with parasites containing >1 copy of the *plasmepsin II* gene ($n = 34$) compared with patients with a single copy of this gene was 5.59 (95% CI = 1.30–24.06) (Table 2). The unadjusted hazard of recurrence in patients with parasites having the PfCRT 145I mutation ($n = 13$) compared with those with the wildtype F145 was 5.12 (95% CI = 2.10–12.49). The association between PfCRT 145I remained significant after adjusting for parasites having >1 copy of *plasmepsin II* and log-transformed parasitemia at diagnosis (adjusted HR = 4.61; 95% CI = 1.73–12.28) (Table 2). In this dataset, all but 4 parasites had a PfKelch13 propeller mutation, such that the presence of a PfKelch13 mutation was not

significantly associated with recurrence and not included in the final model.

In addition, the mean piperazine IC_{90} was significantly greater in parasites with both the PfCRT 145I mutation and multiple copies of *plasmepsin II*, compared with parasites with amplified *plasmepsin II* and without 145I (linear regression, $P = .03$) and compared with parasites with a single copy of *plasmepsin II* and without 145I (linear regression, $P = .0001$) (Figure 5; Supplementary Table 6). The PfCRT 145I mutation only occurred in parasites with amplified *plasmepsin II/III*.

PfCRT and Other Mutations

Within both the fine-mapping and validation datasets, 46 infections contained parasites with multiple copies of the *plasmepsin II/III* genes, 64% of which did not have the 145I mutation, and 36% of which did have the 145I mutation. In addition, the PfCRT 145I mutation only occurred on a Dd2 PfCRT background (ie, in parasites with mutations at positions 75, 326, 356, and 371), and all parasites with 145I showed a single haplotype in SNPs flanking and in LD with the *pfprt* gene (Supplementary Figure 4). All parasites with PfCRT 145I had the 580Y mutation at the *kelch13* locus, whereas 85% ($n = 23/27$) of parasites with amplified *plasmepsin II/III* but without 145I had 580Y. The PfCRT 97Y and 97L mutations [8] were observed in 4 and 2 parasites, respectively, in the fine-mapping dataset. Position 97 was not associated with piperazine IC_{90} in linear mixed models ($P = .60$). The 97Y mutation was not observed, and the 97L mutation was observed only once in parasites within the

Table 2. Cox Proportional Hazards Models of Time to *Plasmodium falciparum* Recurrence

Variable	Hazard ratio (95% CI)	P value
Plasmepsin II >1	5.59 (1.30–24.06)	.02
PfCRT 145I	5.12 (2.10–12.49)	.0003
Plasmepsin II >1	4.14 (.89–19.37)	.07
PfCRT 145I	4.61 (1.73–12.28)	.002
Parasitemia at diagnosis	1.53 (1.00–2.36)	.051

Abbreviation: CI, confidence interval.

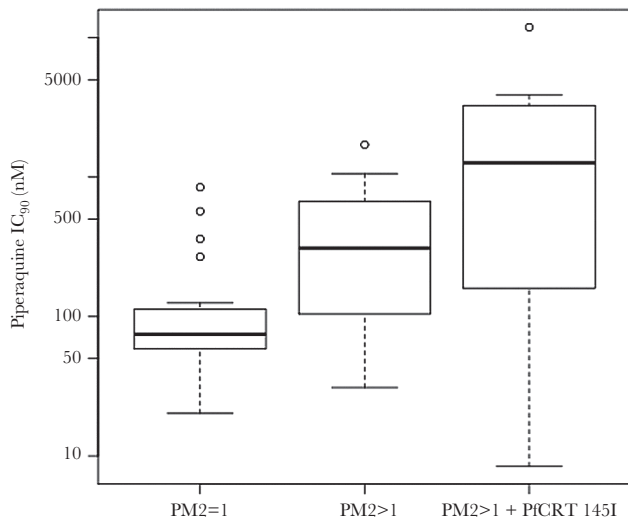


Figure 5. Distribution of piperazine 90% inhibitory concentrations (IC_{90}) among parasites with different combinations of amplified *plasmepsin II* copy number and PfCRT 145I. Box plots indicate the distribution of piperazine IC_{90} in parasites from the validation data set ($n = 53$) in the following groups: parasites with a single copy of *plasmepsin II* and without the PfCRT 145I mutation (*left*), parasites with >1 copy of *plasmepsin II* and without PfCRT 145I (*center*), and parasites with >1 copy of *plasmepsin II* and with PfCRT 145I (*right*). The PfCRT 145I mutation only occurred in parasites with amplified *plasmepsin II* copy number. Abbreviation: IC_{90} , 90% inhibitory concentration.

validation dataset. No parasites in either dataset had mutations at PfCRT positions 343 and 353, positions implicated in a previous study of piperazine susceptibility conducted in a different region of Cambodia [8].

DISCUSSION

Amplification of *plasmepsin II/III* is associated with decreased piperazine sensitivity and may serve as a useful marker for surveillance [12, 13]. We performed a genome-wide association study of ex vivo *P. falciparum* susceptibility to piperazine to identify loci that are associated with decreased sensitivity. Single nucleotide polymorphisms on multiple chromosomes were associated with piperazine IC_{90} in a genome-wide analysis. Fine-mapping of genomic regions implicated in genome-wide analyses identified multiple SNPs in LD with each other that were significantly associated with piperazine IC_{90} , including a mutation within the *pfprt* gene. This mutation (PfCRT F145I) was associated with *P. falciparum* recurrence following treatment with dihydroartemisinin-piperazine after adjusting for the presence of multiple copies of the *plasmepsin II* gene. Although *plasmepsin II/III* copy number was associated with piperazine IC_{90} and dihydroartemisinin-piperazine treatment outcome, our data suggest that other loci may also be involved in resistance.

Amato and colleagues recently reported an association between a mutation within an exonuclease on chromosome 13 and piperazine IC_{50} [35]. We did not see any evidence of an

association between piperazine IC_{50} or IC_{90} and SNPs on chromosome 13 in our genome-wide analysis. We did, however, see some overlap in SNPs identified in the Amato study and regions of the genome identified in our genome-wide analysis, including SNPs on chromosome 12 (MAL12:1787279) and chromosome 14 (MAL14:2385550, MAL14:2395752, and MAL14:2411942). Wang and colleagues [36] also showed an association between piperazine IC_{50} and an SNP in a similar region of chromosome 12 (MAL12:1959796), as well as an SNP on chromosome 8 (MAL8:280180) that is in a region of the chromosome identified in our genome-wide analysis. Although these regions of chromosomes 8, 12, and 14 did not show significant associations in our fine-mapping analysis of whole genome sequences, they were identified in multiple studies and thus warrant further investigation.

We observed a large region of LD on chromosome 10 that was associated with piperazine IC_{90} , both in the regression and random forest analyses. This pattern is consistent with a selective sweep localizing to this region of the genome, which harbors 54 genes (chromosome 10: 1318156–1552425). Of these 54 genes, 9 (PF3D7_1033000, PF3D7_1034000, PF3D7_1034700, PF3D7_1036300, PF3D7_1036400, PF3D7_1036800, PF3D7_1037300, PF3D7_1037500, PF3D7_1038100) had gene ontology terms suggesting a function in hemoglobin metabolism, drug response, or transport, and 1 (PF3D7_1036300, encoding Duffy binding-like merozoite surface protein 2) has been implicated in resistance to halofantrine, mefloquine, and lumefantrine [37]. However, none of these 9 genes had polymorphisms that were significantly associated with piperazine IC_{90} in our fine-mapping analysis of whole-genome sequences. This region of the genome is also in LD with PfCRT F145I, so it is not clear which mutations are driving the signal, but it is possible that additional loci within this region of chromosome 10 are contributing to decreased sensitivity.

PfCRT has been implicated in previous studies of piperazine susceptibility, supporting our evidence that variants of this transporter can contribute to resistance to this chloroquine-like bisquinoline. Specifically, PfCRT 101F was identified in Dd2 parasites exposed to continuous piperazine pressure that had elevated piperazine IC_{50} s [38], and this mutation was able to mediate piperazine resistance in vitro when introduced via gene editing into Dd2 parasites [23]. Mutations at PfCRT positions 97, 343, and 353 have also been associated with decreased piperazine sensitivity [8]. In our datasets, mutations at PfCRT position 97 were not associated with piperazine IC_{90} , and no mutations were observed at positions 343 and 353 in either the fine-mapping or validation datasets.

In this study, we only observed the PfCRT 145I mutation in samples collected from Oddar Meanchey province in the years 2013–2014. Because samples were not available from other provinces for these years of the study (Supplementary Table 7), it is not possible for us to determine the distribution of this

mutation in other regions of Cambodia, which is a limitation of the study. This mutation was not noted in other studies of piper-
aquine susceptibility that used clinical samples from Cambodia [12, 13]. Although these studies did not sample isolates from Oddar
Meanchey province, they did include isolates from neighboring
Preah Vihear province. Future studies will examine the distribu-
tion of PfCRT 145I in other geographic regions and its association
with dihydroartemisinin-piper-
aquine treatment efficacy.

The PfCRT 145I mutation was only observed in parasites
with amplified *plasmepsin II/III* copy number, suggesting that
perhaps in nature this mutation has only occurred or only
attains high frequency on a background of amplified *plasmepsin*
II/III. This observation could suggest that 145I has emerged on
a background of resistance and that its association with resis-
tance is not causal. However, this scenario is not supported by
the observation that the association between PfCRT 145I and
treatment outcome remained significant after adjusting for the
presence of amplified *plasmepsin II/III*. Moreover, the mean
piper-
aquine IC₉₀ was greater in parasites with both amplified
plasmepsin II/III and PfCRT 145I compared with parasites with
just amplified *plasmepsin II/III*, suggesting that 145I results in
an additional resistance effect beyond that caused by ampli-
fied *plasmepsin II/III*. Experiments to introduce PfCRT 145I
into parasites both with and without elevated *plasmepsin II/III*
copy number and to remove this mutation from parasites with
elevated copy number will be important for understanding the
independent effect of the PfCRT 145I mutation and examin-
ing any interaction between this locus and the *plasmepsin II/*
III genes.

Supplementary Data

Supplementary materials are available at *The Journal of Infectious*
Diseases online. Consisting of data provided by the authors to
benefit the reader, the posted materials are not copyedited and
are the sole responsibility of the authors, so questions or com-
ments should be addressed to the corresponding author.

Notes

Disclaimers. Material has been reviewed by the Walter
Reed Army Institute of Research. There is no objection to its
presentation and/or publication. The opinions or assertions
contained herein are the private views of the author, and are
not to be construed as official or as reflecting the views of the
US Department of the Army, the US Department of Defense, or
the US government. In addition, the contents of this publica-
tion do not necessarily reflect the views, opinions, or policies of
Uniformed Services University of the Health Sciences.

Financial support. This research was supported by grants
from the National Institutes of Health (R01 AI101713 and R01
AI125579 to S. T.-H.); R01 AI089819 to J. J. J.; R01 AI124678,
R01 AI109023, R01 AI50234 to D. A. F.; and U19AI110820 to
C. Fraser [project leader J. C. S.]).

Potential conflicts of interest. All authors: No reported con-
flicts of interest. All authors have submitted the ICMJE Form
for Disclosure of Potential Conflicts of Interest. Conflicts that
the editors consider relevant to the content of the manuscript
have been disclosed.

References

1. Denis MB, Tsuyuoka R, Lim P, et al. Efficacy of arte-
mether-lumefantrine for the treatment of uncomplicated
falciparum malaria in northwest Cambodia. *Trop Med Int*
Health **2006**; 11:1800–7.
2. Denis MB, Tsuyuoka R, Poravuth Y, et al. Surveillance of
the efficacy of artesunate and mefloquine combination
for the treatment of uncomplicated falciparum malaria in
Cambodia. *Trop Med Int Health* **2006**; 11:1360–6.
3. Lwin KM, Imwong M, Suangkanarat P, et al. Elimination of
Plasmodium falciparum in an area of multi-drug resistance.
Malar J **2015**; 14:319.
4. Leang R, Taylor WR, Bouth DM, et al. Evidence of
Plasmodium falciparum malaria multidrug resistance to
artemisinin and piper-
aquine in western Cambodia: dihy-
droartemisinin-piper-
aquine open-label multicenter clin-
ical assessment. *Antimicrob Agents Chemother* **2015**;
59:4719–26.
5. Spring MD, Lin JT, Manning JE, et al. Dihydroartemisinin-
piper-
aquine failure associated with a triple mutant includ-
ing kelch13 C580Y in Cambodia: an observational cohort
study. *Lancet Infect Dis* **2015**; 15:683–91.
6. Amaratunga C, Lim P, Suon S, et al. Dihydroartemisinin-
piper-
aquine resistance in *Plasmodium falciparum* malaria
in Cambodia: a multisite prospective cohort study. *Lancet*
Infect Dis **2016**; 16:357–65.
7. Chaorattanakawee S, Saunders DL, Sea D, et al. Ex vivo
drug susceptibility testing and molecular profiling of clin-
ical *Plasmodium falciparum* isolates from Cambodia from
2008 to 2013 suggest emerging piper-
aquine resistance.
Antimicrob Agents Chemother **2015**; 59:4631–43.
8. Duru V, Khim N, Leang R, et al. *Plasmodium falciparum*
dihydroartemisinin-piper-
aquine failures in Cambodia are
associated with mutant K13 parasites presenting high sur-
vival rates in novel piper-
aquine in vitro assays: retrospective
and prospective investigations. *BMC Med* **2015**; 13:305.
9. Ariev F, Witkowski B, Amaratunga C, et al. A molecular
marker of artemisinin-resistant *Plasmodium falciparum*
malaria. *Nature* **2014**; 505:50–5.
10. Ghorbal M, Gorman M, Macpherson CR, Martins RM,
Scherf A, Lopez-Rubio JJ. Genome editing in the human
malaria parasite *Plasmodium falciparum* using the CRISPR-
Cas9 system. *Nat Biotechnol* **2014**; 32:819–21.
11. Straimer J, Gnädig NF, Witkowski B, et al. K13-propeller
mutations confer artemisinin resistance in *Plasmodium fal-*
ciparum clinical isolates. *Science* **2015**; 347:428–31.

12. Witkowski B, Duru V, Khim N, et al. A surrogate marker of piperazine-resistant *Plasmodium falciparum* malaria: a phenotype-genotype association study. *Lancet Infect Dis* **2017**; 17:174–83.
13. Amato R, Lim P, Miotto O, et al. Genetic markers associated with dihydroartemisinin-piperazine failure in *Plasmodium falciparum* malaria in Cambodia: a genotype-phenotype association study. *Lancet Infect Dis* **2017**; 17:164–73.
14. Noedl H, Se Y, Schaefer K, Smith BL, Socheat D, Fukuda MM; Artemisinin Resistance in Cambodia 1 (ARC1) Study Consortium. Evidence of artemisinin-resistant malaria in western Cambodia. *N Engl J Med* **2008**; 359:2619–20.
15. Jacob CG, Tan JC, Miller BA, et al. A microarray platform and novel SNP calling algorithm to evaluate *Plasmodium falciparum* field samples of low DNA quantity. *BMC Genomics* **2014**; 15:719.
16. Parobek CM, Lin JT, Saunders DL, et al. Selective sweep suggests transcriptional regulation may underlie *Plasmodium vivax* resilience to malaria control measures in Cambodia. *Proc Natl Acad Sci U S A* **2016**; 113:E8096–105.
17. DePristo MA, Banks E, Poplin R, et al. A framework for variation discovery and genotyping using next-generation DNA sequencing data. *Nat Genet* **2011**; 43:491–8.
18. McKenna A, Hanna M, Banks E, et al. The Genome Analysis Toolkit: a MapReduce framework for analyzing next-generation DNA sequencing data. *Genome Res* **2010**; 20:1297–303.
19. Van der Auwera GA, Carneiro MO, Hartl C, et al. From FastQ data to high confidence variant calls: the Genome Analysis Toolkit best practices pipeline. *Curr Protoc Bioinformatics* **2013**; 11:11.10.1–33.
20. Chaorattanakawee S, Lon C, Jongsakul K, et al. Ex vivo piperazine resistance developed rapidly in *Plasmodium falciparum* isolates in northern Cambodia compared to Thailand. *Malar J* **2016**; 15:519.
21. Rutvisuttinunt W, Chaorattanakawee S, Tyner SD, et al. Optimizing the HRP-2 in vitro malaria drug susceptibility assay using a reference clone to improve comparisons of *Plasmodium falciparum* field isolates. *Malar J* **2012**; 11:325.
22. Saunders DL, Chaorattanakawee S, Gosi P, et al. Atovaquone-proguanil remains a potential stopgap therapy for multi-drug-resistant *Plasmodium falciparum* in areas along the Thai-Cambodian border. *Antimicrob Agents Chemother* **2015**; 60:1896–8.
23. Dhingra SK, Redhi D, Combrinck JM, et al. A variant PfCRT isoform can contribute to *Plasmodium falciparum* resistance to the first-line partner drug piperazine. *MBio* **2017**; 8:e00303–17.
24. Alexander DH, Novembre J, Lange K. Fast model-based estimation of ancestry in unrelated individuals. *Genome Res* **2009**; 19:1655–64.
25. Browning SR, Browning BL. Rapid and accurate haplotype phasing and missing-data inference for whole-genome association studies by use of localized haplotype clustering. *Am J Hum Genet* **2007**; 81:1084–97.
26. Miotto O, Almagro-Garcia J, Manske M, et al. Multiple populations of artemisinin-resistant *Plasmodium falciparum* in Cambodia. *Nat Genet* **2013**; 45:648–55.
27. Zhou X, Stephens M. Genome-wide efficient mixed-model analysis for association studies. *Nat Genet* **2012**; 44:821–4.
28. Price AL, Patterson NJ, Plenge RM, Weinblatt ME, Shadick NA, Reich D. Principal components analysis corrects for stratification in genome-wide association studies. *Nat Genet* **2006**; 38:904–9.
29. Breiman L. Random forests. *Machine Learning* **2001**; 45:5–32.
30. Liaw A, Wiener M. Classification and regression by randomForest. *R News* **2002**; 2:18–22.
31. R Core Team. A language and environment for statistical computing. Vienna, Austria: R Foundation for Statistical Computing, **2016**.
32. Barrett JC, Fry B, Maller J, Daly MJ. Haploview: analysis and visualization of LD and haplotype maps. *Bioinformatics* **2005**; 21:263–5.
33. Langmead B, Salzberg SL. Fast gapped-read alignment with Bowtie 2. *Nat Methods* **2012**; 9:357–9.
34. Miles A, Iqbal Z, Vauterin P, et al. Indels, structural variation, and recombination drive genomic diversity in *Plasmodium falciparum*. *Genome Res* **2016**; 26:1288–99.
35. Allison AC. Polymorphism and natural selection in human populations. *Cold Spring Harb Symp Quant Biol* **1964**; 29:137–49.
36. Wang Z, Cabrera M, Yang J, et al. Genome-wide association analysis identifies genetic loci associated with resistance to multiple antimalarials in *Plasmodium falciparum* from China-Myanmar border. *Sci Rep* **2016**; 6:33891.
37. Van Tyne D, Park DJ, Schaffner SF, et al. Identification and functional validation of the novel antimalarial resistance locus PF10_0355 in *Plasmodium falciparum*. *PLoS Genet* **2011**; 7:e1001383.
38. Eastman RT, Dharia NV, Winzeler EA, Fidock DA. Piperazine resistance is associated with a copy number variation on chromosome 5 in drug-pressured *Plasmodium falciparum* parasites. *Antimicrob Agents Chemother* **2011**; 55:3908–16.